International Journal of Robotics and Mechatronics 2018, Vol. 5, No. 1

Solar-Rechargeable Brain-Controlled Wheel-Chair for Paralytic Patients Using Emotiv Epoc+

Ahmad Muhammad Faruk†, A. Bakry Hussein†, Marwan A. Rashed†, Sohair F. Rezeka†, Mohamed El-Habrouk‡

†Department of Mechanical Engineering, Faculty of Engineering, AASTMT University, Alexandria, Egypt

‡Department of Electrical Engineering, Faculty of Engineering, Alexandria University, Alexandria, Egypt

Abstract—This paper presents the mechanical design and construction of the solar power rechargeable brain controlled wheel-chair with signal acquisition, feature extraction, processing and control methods. It provides the research performed on building a relatively cheap solar rechargeable brain controlled wheel-chair. In the proposed system, the authors aim to augment the abilities of handicapped people such as moving from one place to another, standing up, as well as hands-free control through several artificial techniques. In order to accomplish this task, the proposed system reads and analyses the patient's brain waves (EEG signals) and turns them into actions to control the proposed wheel chair for moving and standing.

The signals acquired from the EEG were used after filtration, feature extraction, and classification. Furthermore, the signals are passed to the control system of the wheel-chair which consists of motor drivers and linear actuators. An alternative Joystick input is also present in the proposed system for normal use of the wheel-chair. Processing and control are all handled by an Intel based computer and an Arduino Mega 2560-R3 board. The Integration of the system is based on a PID controller and complementary filters leading to high efficient wheel-chair operation.

The system improves the power efficiency by using two solar panels fitted to the rooftop of the wheel-chair in order to trickle charge the batteries of the wheel-chair when it is present under appropriate solar irradiance for the purpose of extending the operating time of the wheel-chair batteries. This led to almost an extra hour of usage as compared to over three hours of usage without the solar panel. The electrical and mechanical designs were all constrained by economical means as well as market availability. The overall cost of the system was around $2000.

Keywords— electro-encephalogram (EEG), brain control interface (BCI), Arduino Mega 2560-R3, wheel-chair, solar powered, paralytic patients.

DOI: https://doi.org/10.21535/ijrm.v5i1.984

I. Introduction

ONE major requirement for a wheel-chair to be used by a patient is for a user to physically control the wheel-chair through a joystick or other input interface device, which would require a physical motion to be performed by the patient. This is a major drawback for a large number of paralyzed handicaps.

Corresponding author: Ahmad Muhammad Faruk (e-mail: ahmadm.faruk@gmail.com)

This paper was submitted on Oct 23, 2017; and accepted on Oct 23, 2017.

Handicapped people are having difficulty dealing with several normal daily tasks, especially paralyzed patients who have lost the ability to walk or even move their upper and lower limbs. These patients constantly depend on external help from others to perform ordinary locomotion or interact with the environment. In the special case where the patient has complete physical paralysis or higher percent of paralysis, control using muscles becomes difficult or extremely stressful [1].

A Brain–Computer-Interface (BCI) [2] or brain–machine interface [3] uses brain signals to drive external devices. The BCI system uses the brain activity to acquire brain wave signals [4]. These signals are acquired and passed through amplifiers and filters [5]. They are then decoded using classification [6]. A BCI has different forms in which an action can be performed from brain signals [7] such as event-related potentials (ERPs) [8], electroencephalogram (EEG) oscillations [9], extracellular local field potentials (LFPs) [10], near-infrared spectroscopy (NIRS) [11], real-time-functional magnetic resonance imaging (rt-fMRI) [12], spike trains from single neurons [13] and electrocorticography (ECoG) [14]. BCI has many advantages in comparison with modern wheel-chair controls such as ease of use, improvement of the quality of life for patients and reduction of frequent costs for intensive care [15].

BCI research started with animal research in several laboratories to see the effects and applications of BCI [16]. During the research, scientists and engineers managed to record signals from cerebral cortices of animals such as monkeys and mice. These animals have very similar cerebral cortices to humans in order to operate BCI to perform basic movements [17]. Some monkeys successfully navigated cursors on monitors and moved some robotic arms simply by thinking commands about the task and having a visual feedback with their eyes. These were all performed without any muscular movements. In May 2008 photographs that showed a monkey at the "University of Pittsburgh Medical Center" operating a robotic arm by thinking were published in a number of well-known scientific journals and magazines [18].

Experimenting on animals is one thing, but human experiments are entirely different. Certain measures and safety precautions need to be ensured. Based on this condition, methods of applying BCI to human brains is classified under three categories [19]:

1. Invasive BCIs [20]
These are mostly used in vision and movement repair experiments. It involves implanting sensing devices directly onto the grey matter of the brain during neurosurgery. It gives the best signal but causes scar-tissues due to the invasive nature of the device on the brain and can be rejected by the body [20].
2. Partially Invasive BCIs [21]
These types of devices are implanted in the skull but rest outside the brain grey matter. They have a lower risk of scar tissues than the invasive type. There were researches performed on intracortical BCIs from the stroke perilesional cortex [21]. ECoG is similar to non-invasive electroencephalography which measures the electrical activity of the brain taken from underneath the skull but the main difference is that the electrodes are embedded in a thin plastic pad that is placed above the cortex, beneath the dura mater [22]. ECoG has a bright future in BCI modality because it has better spatial resolution, better signal-to-noise ratio, wider frequency range, and less training requirements than scalp-recorded EEG. This feature and evidence of the high level of control shows potential for real world application for people with motor disabilities [23, 24].
3. Non-Invasive BCIs [25]
This type uses a device that is mounted directly onto the patient's head without the need for any neurosurgery [25]. It can be easily removed and mounted for repairs or just change. There have been many experiments on human brain using non-invasive neuro-imaging technologies as interfaces [26]. This type mostly uses EEG for its application of BCI. This is the type used in this research because it possesses non-invasive nature and less risk to the patient. Moreover, the device is also relatively cheaper and easier to acquire than the other types of devices.

The requirements for the proposed wheel-chair should have the following specifications. It can:

- accommodate a patient up to a mass of 120 kg.
- be used to move in all directions.
- be used to change the angle of inclination of the patient from sitting position to fully standing vertical position and to fully stretched horizontal position.
- be controlled using a joystick.
- be controlled using brain waves.
- be used to climb stairs.

This paper presents: (1) the design and fabrication of a motorized wheel-chair reducing cost based on the availability of resources around the world; (2) the demonstration of the use of an EEG device to help paralyzed patients in need of independent locomotion option; and (3) the use of solar panel to conserve energy, minimize cost and increase durability & energy efficiency of the power source in the long run for the motorized wheel-chair.

Section II of this paper describes the proposed wheel-chair detailed mechanical and basic electrical designs used in solving the problem of locomotion for paralyzed patients. Section III presents the electrical system in greater details including the actuator selection, power/supply requirements and solar energy battery power replenishment options. This is followed by Section IV, which gives an overview of data acquisition, signal processing and feature extraction used in this research. Section V describes the overall results from the proposed system stating the successes and challenges of the research. The paper is coroneted by the conclusion in Section IV, which summarizes the research outcome and possible future improvements to this research.

II. Proposed System

This section explains the concept of the mechanical design, and its idea. It also shows a general view for the parts used in the mechanical, control and electrical systems.

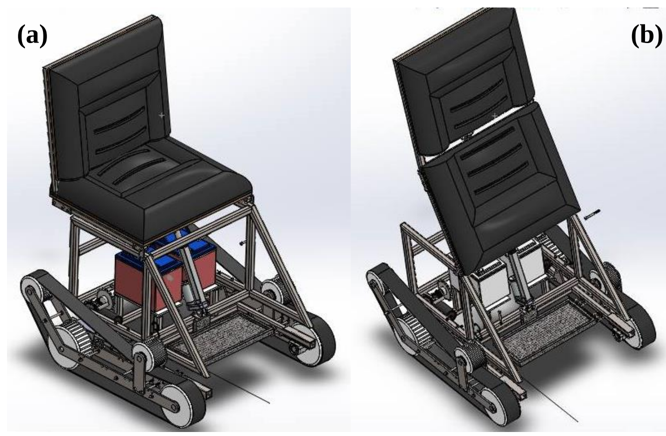

Figure 1: Render images of the proposed wheel-chair: (a) Sitting Position, and (b) Standing Position.

Table 1: Chair dimensions

Chair parts		Dimensions (mm)
Overall chair in sitting position	no solar panels	970×720×1140
	with solar panels	1020×695×1754
Overall chair in standing position	no solar panels	970×720×1620
	with solar panels	1020×695×2234
Seat		440×540×140
Back support		140×540×420
Pulleys	top	D110×78
	bottom	D150×78
belt		2000×70

The proposed wheel-chair, shown in the various render images of Figure 1 for the mechanical part only, uses a track-based wheel system instead of regular circular wheels. Since the wheel-chair has the capability of climbing up and down a stair case, a belt system was chosen since it is suitable for reducing the probability of slipping according to the calculations performed. The belt is mounted on four pulleys, two on top and two at the bottom. These pulleys act as guides to keep the belt in place. The pulleys are made from artelon plastics which is steady and rigid and compatible with the application requirements according to calculations. Chair dimensions are shown in Table 1.

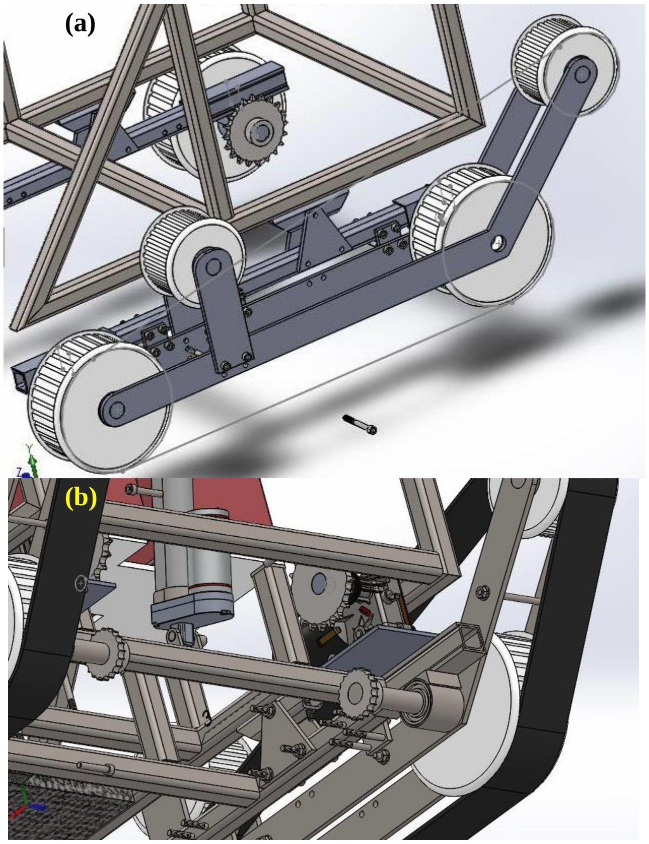

Figure 2 Drive train of the system:
(a) Outside View and (b) Inside View

The drive train of the wheel-chair is rather unconventional for a wheel-chair because it includes extra power transmission systems, as shown in render design images of Figure 2. The motors are mounted on the bottom and close to the center for mass distribution and stability. These motors are connected to small sprocket and chain system. This gives extra room for connection to a larger wheel (pulley). The other end of the chain is then connected to another sprocket fixed to the large rear bottom pulley. Henceforth, the long belt for the tracked wheels transfer power to other pulleys to drive the wheel-chair.

Stress analysis was performed on the wheel-chair with a stainless-steel material having dimensions of 25×25 mm^2 using Solidworks software [27]. The results show that it conforms to the calculations made and are within the safe limits using a factor of safety of 1.2. Stress analysis on other parts and materials such as the drive train and belt (rubber material) were also within permissible limits.

Two powerful 24VDC/12.5A motors were made use of as the source of mechanical rotational power. The motors, of type TDCMLDFZ001 from IMC motors in Taiwan, are similar to the ones used in regular motor-powered wheel-chairs. The power ratings of these motors are more than enough to power the proposed wheel-chair and at the same time, are economical for consumers since they are standard wheel-chair motors that can be bought and serviced like ordinary ones. These motors have a safety feature to prevent damage and injury. This feature is the coupled active-low emergency motor brakes. The brakes lock the shaft of the motor when there is no power to the brake system. It is disengaged only when electric power is applied to it just like the emergency brakes on elevators in case of power failure.

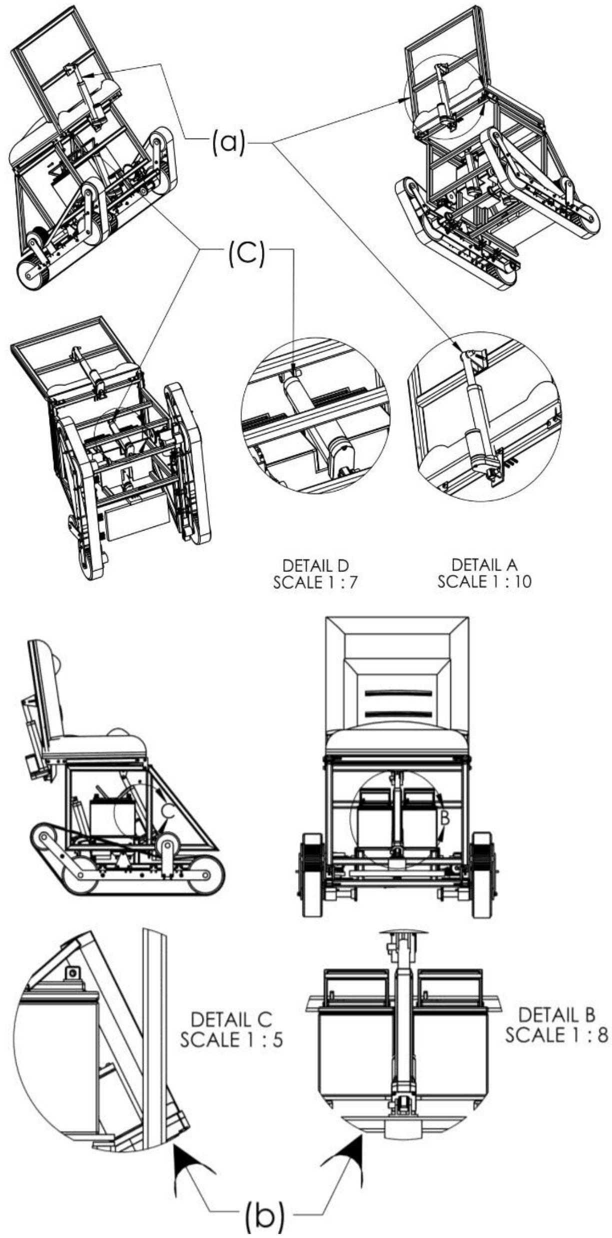

Figure 3 (a) Back seat linear actuator,
(b) Linear actuator seat, and (c) Balancing linear actuator

Aside from the driving motors powering the movement of the wheel-chair, three MH300-A 24VDC/3A/200mm linear actuators with maximum speed of 3mm/sec were also chosen and used. According to Figure 3, each linear actuator has a specific stroke, which is long enough for the dimensions of the wheel-chair according to design. Two of the linear actuators are used in the mechanism for making the patient stand up or sit down (one for the base and one for the back of the wheel-chair). The wheel-chair has the capability of transforming into a chair, a horizontal bed and a standing-support wall for a patient to be fully upright. The third linear actuator is used to stabilize the wheel-chair when climbing stairs.

Each linear actuator is responsible for doing a special function to serve a specific mechanism. The linear actuator shown in Figure 3a rotates the backseat by fixing the linear actuator to the chair frame as shown in Figure 3a. This will not allow the linear actuator to move but its piston only, which is mounted to the backseat. Once the linear actuator is powered on, its piston will move up or down and will drag the backseat with it. This will prepare the back seat for standing/sitting/bed positions. The second linear actuator is mounted right under the seat. Moving the piston upward will let the seat rotate over two hinges as shown in Figure 3b. Mounting the linear actuator and fixing it in such a way that it will allow the seat to rotate as shown in Figure 3b. Mounting and operating the two linear actuators simultaneously in such a way that they will allow the whole seat to stand in the upright position in addition to moving the feet support accordingly as shown in Figure 3b.

As mentioned earlier, the stabilization mechanism was used to avoid shifting of the mass of gravity while climbing stairs. In order to achieve this goal, a linear actuator as shown in Figure 3c was mounted to pitch the seat upward and downward. The piston is mounted in the frame as shown in Figure 3c. When the linear actuator is powered, it rotates the chair around an Allen screw which is mounted on a hinge, which rotates with the seat as shown in Figure 3c.

The wheel-chair can transform and give the patient the ability to stand and sit willingly. This is one of the extra features included in this design. Patients do not like being incapable of performing simple tasks and becoming a burden to others. So, these features would allow them to be independent and have the freedom to do more on their own, especially when fully standing up.

The problem is that not all buildings and locations include ramps for wheel-chair based people, but staircases on the other hand, are common in all high rising buildings. This is why a climbing system mechanism was included into the proposed design to make it convenient for the patient to move up and down a stair case. The smaller rear pulley at the top of the track is used to move the chair up since it is inclined to the angle of the standard staircase. Since climbing the staircase tilts the wheel-chair, the third linear actuator corrects this tilt to support the patient. This is effectuated by changing the inclination angle of the wheel base. This is performed in order to prevent the patient from falling when going up or down a staircase. Despite the fact that this was included in the mechanical design, the control system to make use of this property is not presented in this paper and will be the subject of a different publication along with the analysis of the stability measures taken for balancing both the patient and chair in such inclined positions.

This research presents a control system using an Arduino Mega 2560-R3 [28] in conjunction with an Intel based laptop in order to perform the signal acquisition, signal processing and control tasks required for this research. The Arduino Mega 2560-R3 is a single-board microcontroller that uses Atmel AVR microcontroller to provide users with necessary components for simple control. It is distributed as open-source hardware and software, which are licensed under the GNU Lesser General Public License (LGPL) or the GNU General Public License (GPL) [29].

In this proposed system, the Arduino Mega 2560-R3 was used instead of a more complex Raspberry pi microcontroller board due to the fact that the control process required to be performed for this specific research presented herein is simple and does not require the sophistications and the high processing power of the Raspberry pi system, which is capable of running a full operating system. Mini-computers can also be an even more powerful system implementation than the control devices presented in this research allowing the application of heavy duty processing algorithms for the EEG signals as well as the wheel-chair balancing algorithms. This will be included in future publications.

To run the proposed motorized wheel-chair, a very reliable power source was needed that is cheap, stable, safe, convenient, and is able to run for extended periods of time. This is why two 12V/35Ah rechargeable sealed Calcium batteries were used and connected in series to provide both 12 V and 24 V. These voltages are required by the three 24V-actuators and the two 24V-driving motors as well as the generation of the 5 V for the embedded micro-controller. This will be explained later on in the course of this paper.

To recharge the batteries, either a dedicated rectified AC power supply is used to charge them or a conveniently mounted solar panel on top of the wheel-chair. This solar panel serves a dual purpose. It acts as a source of electric energy to supply the trickle charging of the batteries in case the system is operating outdoors in a sunny environment as well as a shield for the paralyzed person on the chair from the solar rays.

Solar panels have varying and limited efficiencies depending on their application [30]. The efficiency of a module determines the area of a module given the same rated output [31]. For example, an 8% efficient 230W module will have twice the area of a 16% efficient 230W module [32]. There are few commercially available solar modules that exceed efficiency of 22 % and reportedly also exceeding 24 % [32]. It is henceforth required to use the highest possible efficiency solar panel in order to benefit from the largest amount of power required for the system to operate. The solar panel chosen is a 50W rated mono-crystalline solar panel.

III. Electrical System Design

This section presents function and the selection of the actuators used in the proposed wheel-chair design and implementation. It also analyses the power consumption of the overall system and shows each electrical machine consumptions, as well as the battery power charging and discharging requirements and conditions. It also presents the solar energy battery replenishment system option.

A. *Linear Actuator Selection*

Linear actuator selection depends mainly on torque, and stroke. However, there are many other characteristics like: Voltage, No-Load Speed, Full-Load Speed, No-Load Current, Noise levels, Maximum duty cycle, Life expectancy, etc. [33]. In addition, a major factor of selection in such cases is the economic cost of the actuator itself and its suitability to the application. The main focus in this section is given to torque and stroke.

1) Torque

There are three different mechanisms, where the use of linear actuators is mainly required. Since the wheel-chair was designed for 120 kg, the selection of linear actuators to fit the stresses generated from the mass at the various designed positions of the motion of each one of these actuators in order to achieve the desired tasks.

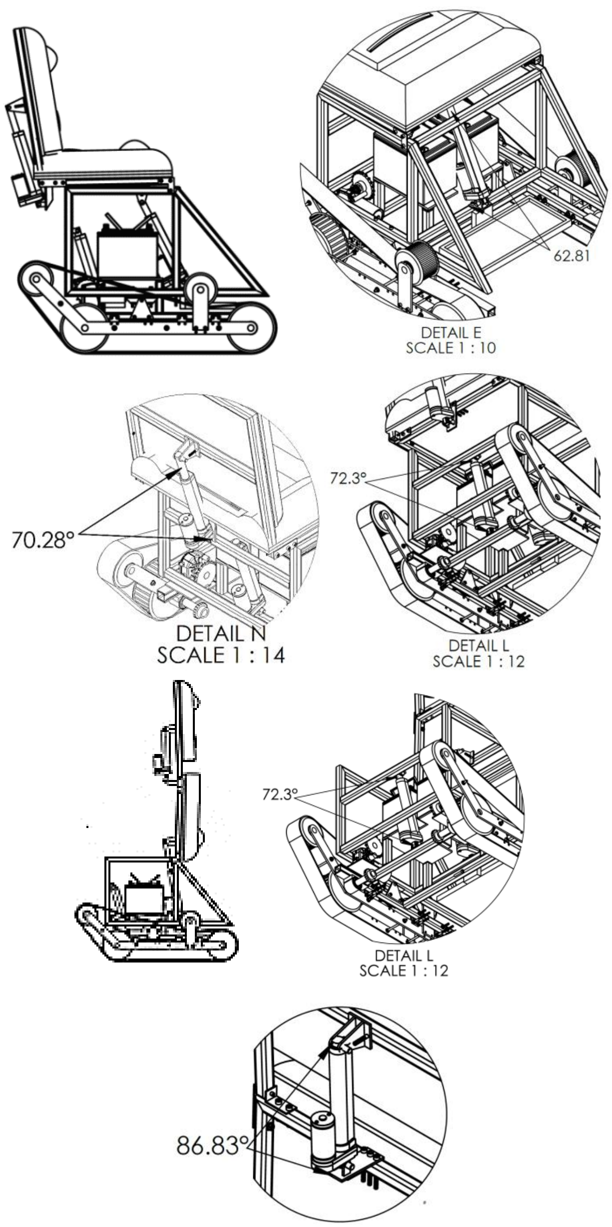

Figure 4 Inclination angles of the actuators and motors (arrows indicate axes of the angles)

To calculate torque required, it is mandatory to find the distance between the mass affecting and the top of the piston multiplied by the force affecting the linear actuator [34]. Since each mechanism has its own torque requirements, the difference will be the angle (theta) between the piston and the linear actuator fitter, and the height. This is clearly depicted in Figure 4. The angle cannot exceed 90 degrees and in the proposed design, it will never exceed 45 degrees. The lesser the angle theta will be, the lesser torque will be required.

The calculations of maximum and minimum theta angles in degrees, heights in meters and torques in Nm are presented for the three actuators of Figure 3 in Table 2 below, which shows the results of these calculations.

Table 2: Maximum and minimum calculations of Theta and Torques for the three mechanisms under study

	Theta (degrees)		Height (m)		Torque (Nm)	
	Max	Min	Max	Min	Max	Min
Figure 3a	86.83	70.28	0.2535	0.2178	328.387	266
Figure 3b	72.3	62.81	0.1967	0.1086	249.878	125.328
Figure 3c	82.5	65	0.1022	0.1636	131.46	33.404

From Table 2, the largest value of 1500 Nm was selected for marketing purposes. The factor of safety used in this case was 1.2, which is relatively low and should be increased. The cost of the motors would escalate with higher factors of safety. This in effect is a case for economical consideration when this proposed wheel-chair is practically implemented. It would only affect the power ratings of the system and the power consumption, which is directly proportional again to the cost of the overall system.

2) Stroke

Due to the free space, available around each one of the three linear actuators, the same stroke was chosen for all the linear actuators. This value was chosen to be 200 mm from the largest value available in Table 2. This value is readily available in the market at the required torques chosen above.

The fact that the three actuators are exactly identical is a very useful point to consider from the point of view of maintenance since the dealer would only have to stock only one rating for all the actuators.

B. Electrical Systems Consumption

This calculation will be divided into two parts:

- ➢ At no load when mounted on the chair without a patient
- ➢ At full load when mounted on the chair with a 120 kg patient

Table 3: Electrical characteristics of the system components

	Current (A)		Operating Voltage (VDC)	Power (W)
	min.	max.		max.
Wheel Motor 1	6.5	12.5	24	300
Wheel Motor 2	6.5	12.5	24	300
Seat Actuator	0.5	1.2	24	28.8
Back Seat Actuator	0.5	0.8	24	19.2
Stabilization Actuator	0.75	1.5	24	36
Electronic Components	---	1	5	5
Total Required	---	29.5	---	689

To achieve this calculation, one must classify the electrical devices in the proposed system according to Table 3. This table shows the current and power consumption of each of the above components outlined.

The maximum loading currents of these loads would of course be variable during the chair operation due to the different loading conditions of the chair at the different positions and speeds. Only maximum values are considered here for the design as a safety measure.

The total power consumption outlined in the above table (689 W) considers of course that all the systems would be operational at the same time with a diversity factor of 1. This is not the case, which implies that the system consumption would not be as much as the value outline above. Nevertheless, a factor of safety of 1.2 is used for the electrical loading conditions [35] which in this case amounts to 826.8 W. The maximum current drawn by the system is 29.5 A. If this value is multiplied by a factor of safety of 1.2, the resulting maximum current would be 35.4 A. Of course, all loads would not be operational at the same time as outlined earlier, which accounts for an additional factor of safety of the electrical system design.

C. Battery Selection

Depending on the maximum ratings calculated above, a suitable battery to provide the efficient power for the whole system is to be selected. The design current is taken to be 35 A. As mentioned earlier, the suitable battery system to accommodate two voltages of 12 VDC and 24 VDC is to use two 12VDC batteries to be connected in series. The rating of each of the two batteries was chosen to be 35 Ah. The type of battery decided upon considering cost and operational characteristics was a sealed battery due to its relatively cheap price as compared to its long life-cycle and its sufficient rating.

The batteries used herein are two batteries of type CMF (Calcium Premium Battery) 40B19L. Each battery is rated at 12V/35Ah with a cold cranking current of 330 A. As mentioned, the two batteries are to be connected in series to achieve the 24 V and two tapings would enable the simultaneous operation of the 12V and 24V systems. The 5V is generated from the 12V using the regulator on-board the Arduino Mega 2560-R3 system used.

The main problem with batteries is of course that they run out of energy after being used for a certain time. This time (discharge time) is determined by the loading conditions and the rate of utilization of the user. For convenience, batteries should be able to run for at least a couple of hours [36]. The charging of the battery (or batteries in this case) would require a connection to the specific charging circuit suitable for the type of battery. The wheel-chair in this case would be rendered impractical being attached for a prolonged period of time to the charging circuit. The solution proposed in the following sub-section would be of course to charge the batteries using solar panels. However, this process has its own restrictions as explained in the following sub-section.

D. Solar Panels

The solar panel would add a means for the wheel-chair to be charged with a cheap and clean energy source while it is present outdoors in sunny environments. Moreover, the wheel-chair would not be stationary next to its dedicated charging circuit for prolonged periods of time. However, charging on the go is not easy since the current and hence power requirements from the supply are relatively large from the point of view of a solar panel of the suitable dimensions to the chair.

The horizontal chair dimensions are 970 mm × 720 mm. This would incur that the solar panel dimensions be as similar as possible. The possible surface area of the solar panel in this case would be in the range of 0.6984 m^2. This area would imply that the maximum rating of the solar panel suitable would not be enough to generate the total current/power requirements needed for the system operation. The only feasible solution would then be to use the solar panel to partially charge the batteries and not to supply the overall rating of the system.

Table 4: Specifications of each one of the two mono-crystalline solar panel used in the proposed system [38]

Parameters	Mono-Crystalline Solar Panel Specifications
Nominal Power (Pmax)	50 W
Voltage (Vmp)	18 V
Current (Imp)	2.8 A
Voltage Open Circuit (Voc)	22 V
Short Circuit Current (Isc)	3 A
Module Size	720×540×30 (mm×mm×mm)
Module Weight	4.4 kg
Max. System Voltage	1000 V
Standard Test Condition	AM1.5, 25C. 1000 W/m^2

The selection of the solar panel was based on the physical dimensions mentioned above and the market research conducted on the local market at the time of this research. The solar panel chosen for the propose system is a 50 W rated mono-crystalline solar panel [37]. Two of these panels would be used and fitted together. They would be connected in series in order to generate enough voltage to charge the two batteries together (24 VDC). The specifications of each one of the solar panels are summarized in Table 4. The terminal characteristics of each one of the solar panels used are presented in Figure 5.

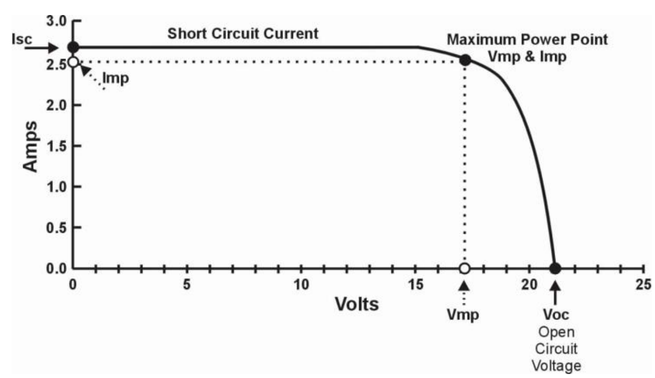

Figure 5 Solar panel terminal characteristics

Table 5: Specifications of Wellsee MPPT solar charge controller used in the proposed system [38] along with the settings adopted

Parameters	Wellsee MPPT controller WS-MPPT30	Setting Adopted
Rated Voltage	12V / 24V	24V
Max Load current	30A	30A
Input voltage range	12V~20V / 24V~40V	24V~40V
Charge loop drop (Length ≤ 1 m)	0.25V	---
Discharge loop drop (Length ≤ 1m)	0.05V	---
Over voltage protection	17V / 34V / 48V	34V
Full charge cut	13.7V / 27.4V	27.4V
Low voltage cut	10.5~11V / 21V~22V	21V~22V
Temperature compensation	-3mv/ °C/ cell	---
No load loss	≤10mA	---
Max wire area	4 mm2	---
Ambient temperature	-25°C to +55°C	---

The above two series connected solar panels require an efficient charger capable of handling a suitable charging current within the limits of the panel, in addition to enabling the load supply with the required current for its safe operation. In addition, it should be able to provide smooth and stable charging of the batteries of the wheel-chair. This task is handled by the Wellsee Maximum Power Point Tracking (MPPT) controller WS-MPPT30 solar charger controller model (TD30) [39]. The specifications of the MPPT charge controller are illustrated in Table 5 along with the settings adopted for the control process in this case.

The MPPT charge controller has 6 terminals which are used as input and outputs. The first 2 terminals are for connecting the solar panel terminals as inputs to the controller. The second pair is for the connection of the batteries to the controller. Finally, the last two terminals are for the output direct to the motors load [40-41].

The MPPT charge controller with an input of 24 V to 36 V from both series connected solar panels can generate an output sufficient to charge both of the 12V batteries used in series in the system.

Please note that the electronic circuits of the control system are permanently connected to the first battery (12 V which is later converted to 5 V inside the Arduino Mega 2560-R3 board). It is worthwhile to note here that the two 24V motors and the three 24V actuators are connected directly to the output of the charge controller. The charge controller output is set to work in current control mode.

The two solar panels are physically mounted on the top of the back support of the wheel-chair at an angle of 90 degrees to the vertical axis. The solar panels are not attached to any linear actuator but are mounted in a static position. They are fixed to the back of the seat. As the wheel-chair transforms from a position to any other position, the back-support movement takes into consideration the angle of the attached solar panel to avoid hitting the patient or other surfaces. This is clearly depicted in Figure 6.

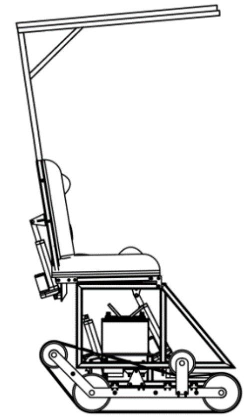

Figure 6 Solar panel fixation

IV. Data Acquisition, Signal Processing, and Feature Extraction

Electroencephalography (EEG) can be defined as an electrophysiological method of monitoring the electrical changes in the brain [42]. It is a non-invasive method of measuring voltage changes as a result of ionic currents within the neuron of the brain [43]. There are few EEG sensors in the market such as Neurosky Mindwave [44], Muse [45], Emotiv Epoc+ [46]. After a considerable market research and comparison of the best sensor suitable for this research from the point of view of availability, ease of use and cost, the "Emotiv Epoc+" was chosen and used to read the EEG signal from the brain.

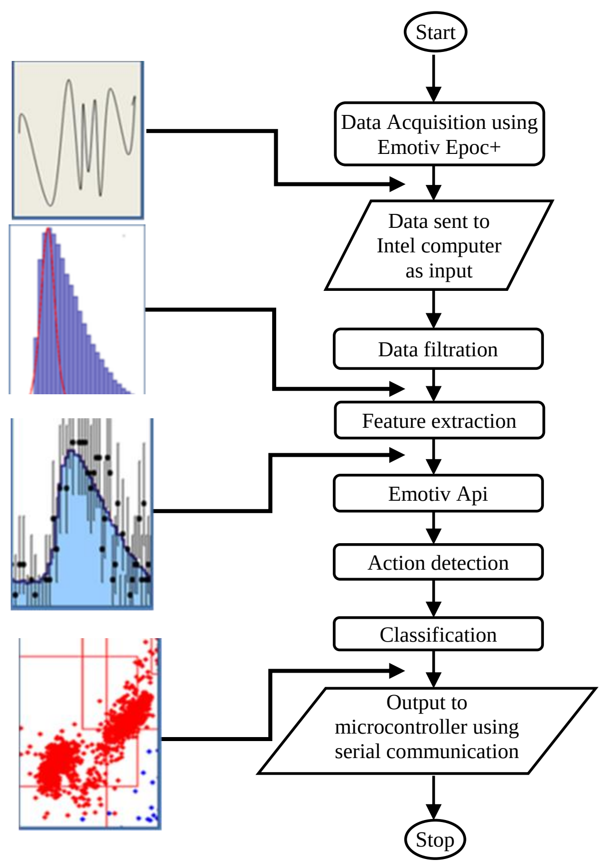

Figure 7 EEG processing block diagram

Emotiv Epoc+ [46] is a 14-channel wireless EEG headset used for EEG signal acquisition from the scalp of the brain. The Emotiv Epoc+ headset has become popular as a result of its low-cost and features [47]. The 14 electrodes are AF3, AF4, F3, F4, FC5, FC6, F7, F8, T7, T8, P7, P8, O1, O2 plus two standard reference electrodes (CMS, DRL). In addition, the sensor incorporates a gyroscope, which provides information about head movements [47]. The Emotiv Epoc+ has two different sampling rates, namely 128 or 256 samples per sec per channel. The Emotiv EPOC+ headset has other useful features such as detecting different facial expressions. Emotiv Epoc+ also comes with some useful software for processing and visualizing the EEG live signal [48].

The most important steps of the EEG processing control method are:

- data acquisition step,
- data processing step, and
- feature extraction step.

These steps are shown clearly in Figure 7. The explanation of each of the above steps is discussed in the following sub-sections.

A. Data Acquisition

By definition, Data acquisition is the process of obtaining data from the real world physical quantities through a sampling process of a particular signal and then converting the sampled data into numerical values that a digital computer can understand and manipulate [49] (Figure 8). In order to get the mental commands from the brain, one needs to find a physical quantity to be measured and analyzed. When a mental command is uttered, a small electrical signal (Voltage) is released from the synapses of the brain (EEG Signals). These EEG signals are what will be used to determine mental commands since they are unique for each separate command [50].

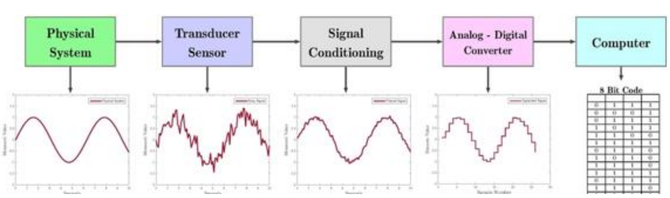

Figure 8 Digital Data Acquisition System Block Diagram [49]

Using Emotiv EPOC+ commercial BCI device as a form of data acquisition device, provides the experiment with the EEG signals from the brain. The EEG signal is sent from the head mounted device wirelessly via a dongle/Bluetooth signal to the microprocessor and then to a software for processing. The default sampling frequency of the device of 128 Hz was used (i.e. a sample was taken every 7.8125 ms). This was sufficient enough for the four frequency bands which contain the valuable Event Related Potentials (ERPs) information, (Nyquist rate = 128/2 = 64 Hz) [51-53].

The Emotiv EPOC+ headset was prepared before placing the electrodes on the user's head. One of the advantages of the Emotiv EPOC+ headset is that the preparation time is much less than other EEG headsets [54]. It takes about 2 to 3 minutes as compared to other EEG headsets which require more than 10 minutes for preparation step [47]. A few drops of saline liquid were applied to wet the sensors and reduce the electrodes impedance. It is important to check the contact quality before starting the acquisition step. To check the quality of the sensors connection, a software called the Emotiv Xavier SDK [55] is run. The Emotiv Xavier SDK panel has many functions one of which is to provide feedback to the user about the contact quality for each sensor on the Emotiv headset. The Emotiv Inc. company suggests some steps to improve the contact quality when problems are detected [55]. To improve the contact quality, the headset should be fully charged. The incorporated Lithium battery can be fully recharged in approximately 4 hours [56]. In addition, more drops of saline solution should be added on each felt (sensor electrode tip) [57]. Moreover, sensors must be fitted properly in order to be in good contact with the head [58].

B. Signal Processing

Signal processing is defined as the manipulation, analysis, modification and synthesis of a signal [59]. In nature, the physical quantities almost always come with noise and extra steps must be taken to ensure the desired signal is obtained by eliminating all other unrequired signals (noise) through a process known as Signal Filtration [60] as depicted in Figure 9 reproduced from [61] for convenience.

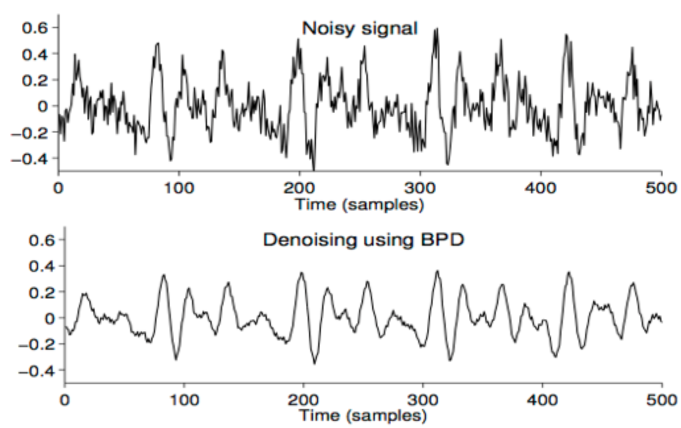

Figure 9 Filtering a noisy waveform using basis pursuit denoising (BPD) [61]

Various signal processing techniques and machine learning algorithms were developed to increase the reliability of the P300-BCI speller system [62]. To classify the target and non-target signals, different classification algorithms have been implemented successfully such as Step-Wise-Linear Discriminant Analysis (SWLDA) [63], Independent Component Analysis (ICA) [64], Support Vector Machine (SVM) [65], etc. In this research, Emokey [66] and Openvibe [67] platforms were used, which provide two different classification algorithms [68]: Linear Discriminant Analysis (LDA) and Support Vector Machines (SVMs) [65].

C. *Feature Extraction*

Feature extraction is the extraction of a relevant portion of a signal associated with a mental task [69]. In the simplest form, a certain frequency range is selected and the amplitude relative to some reference level is measured. Typically, the features are certain frequency bands of a power spectrum. The power spectrum (which describes the frequency content of the EEG signal) can be calculated using, for example, Fast Fourier Transform (FFT) [70].

No matter what features are used, the goal is to form a distinct set of features for each mental task. Feature extraction is highly subjective in nature. It all depends on what type of problem is being handled [69]. There is no generic feature extraction scheme which works in all cases [71]. If the feature sets representing mental tasks overlap each other too much, it is very difficult to classify mental tasks, no matter how good a classifier is used [72]. On the other hand, if the feature sets are distinct enough, any simple classifier can classify them [73].

There are many algorithms for signal decoding and feature extraction such as Discrete Fourier Transform (DFT) [74], Fast Fourier Transform (FFT) [70], Discrete Time Fourier Transform (DTFT) [75], Wavelet Transform [76] and many more.

The Emotiv Emokey [77] software, shown in Figure 10, was used in the proposed system. It is a free software that takes care of the data processing and feature extraction steps. The software gives various mental commands, shown partially in Figure 11, that can be mapped to keyboard keys or that can be used to launch and control applications in a computer.

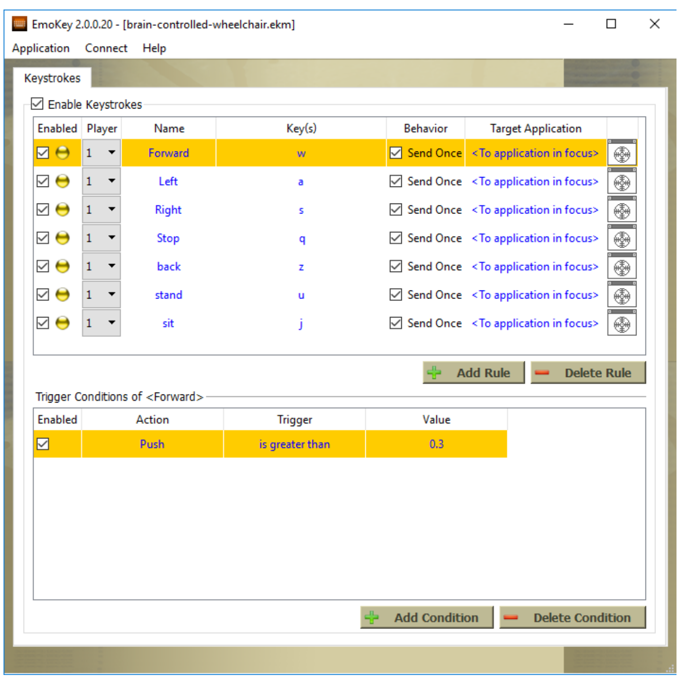

Figure 10 Emokey with mental commands assigned to specific actions

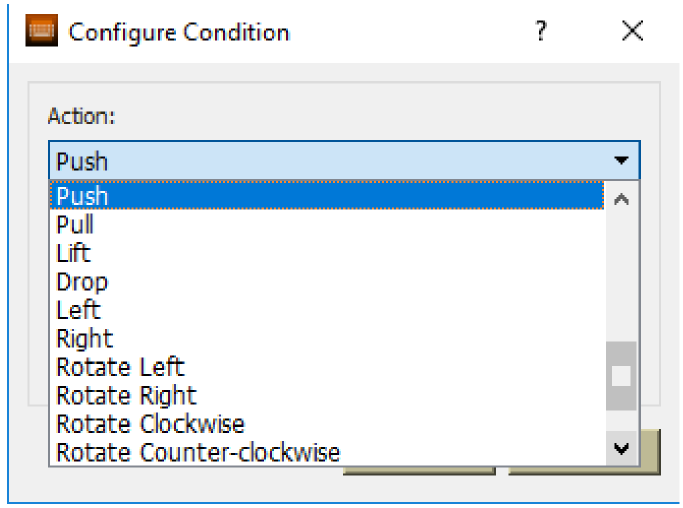

Figure 11 Mental commands available for training and assignment

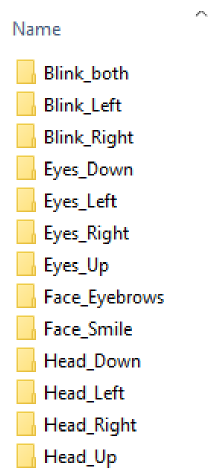

Figure 12 13-mental commands used

A user needs to train with the brain sensor using Emotiv Xavier software to be able to allow the software to identify the unique features for individual users. Other forms of experiments were also used to determine the features required for each user. After obtaining about 1820 electrodes samples, MATLAB R2016a [78] software was used to analyze and extract features from the EEG signal to better optimize Emokey. For each of the 13 mental commands identified, 10 different samples were recorded with varying conditions. The 13 mental commands adopted are shown in Figure 12. For each of those 10 different samples, the signal from each of the 14 electrodes was analyzed independently and in various combinations by transforming the time domain signal into an FFT signal to determine the underlying frequencies of the signal. Using the built-in filters in MATLAB, noise and unwanted frequencies were removed and filtered such as the 50-60 Hz of the 220 V power supply. An example of the time and frequency domain signals measured and analyzed is shown in Figure 13.

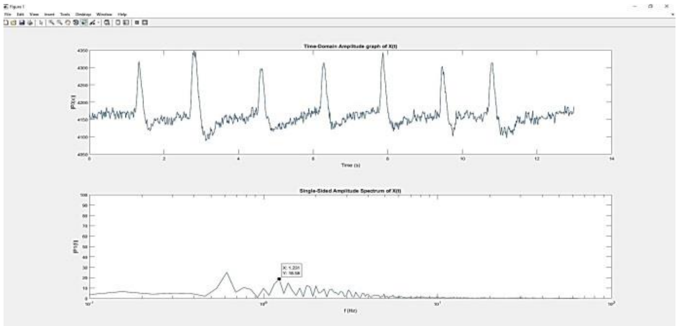

Figure 13 A single electrode graph showing the time domain signal and the frequency domain signal

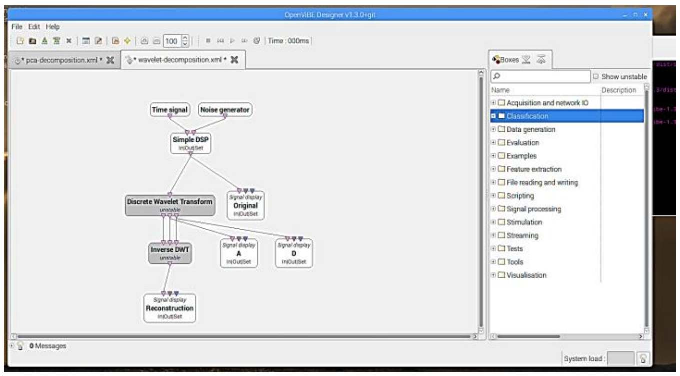

Figure 14 Signal processing using OpenVIBE

Other processing application were also explored, especially OpenVIBE [79], which is an open-source software for BCI applications. It uses a graphical form of programming using blocks and connecting lines for fast and easy programming, as shown in Figure 14. It was used to test the proposed FFT algorithm on a real-time time frame. The advantage of using OpenVIBE is in the fields of application. These fields include medical (assistance to disabled people, real-time biofeedback, neurofeedback, real-time diagnosis), multimedia (virtual reality, video games), robotics and all other application fields related to brain-computer interfaces and real-time neurosciences. Moreover, OpenVIBE users can either be programmers or people not familiar with programming. This includes medical doctors, video game developers, researchers in signal-processing or robotics, etc.

V. Experimental Results

Building the mechanical parts of the wheel-chair took place in the Arab Academy for Science, Technology and Maritime Transport (AASTMT) workshop using the machineries available in the university. The overall cost of the system reached around $2000. After manufacturing and assembling all parts, each subsystem was tested according to the designs and calculations. Finally, each tested configuration (sitting, standing or flat horizontal) turned out to be successful after a few iterations due to manufacturing inaccuracies. The assembled system is shown in Figure 15 from several viewing angles and for the different parts of the system before and after the fixation of the solar panels on top of the patient's head.

Figure 15 (a) Assembled prototype from several viewing angles without solar panel; (b) Assembled prototype from several viewing angles with solar panel

During the testing process, the user was seated on the wheel-chair and the Emotiv Epoc+ device was mounted on his shaved head for better data reading. The user was instructed to focus his attention to the command he wished to utter. In addition, the user was asked to meditate, relax and avoid unnecessary movements to collect useful data for processing and testing in different conditions.

It is worthwhile to know that every subject has unique EEG signals and so as mentioned earlier, a solution might work for one person but not for another. This would imply the necessity for training and tuning process for each new user. The technique used in this case would be the subject of another publication. A sample of the EEG signal captured by the Emotiv Epoc+ is shown in Figure 16 for all the 14 sensors available in the device.

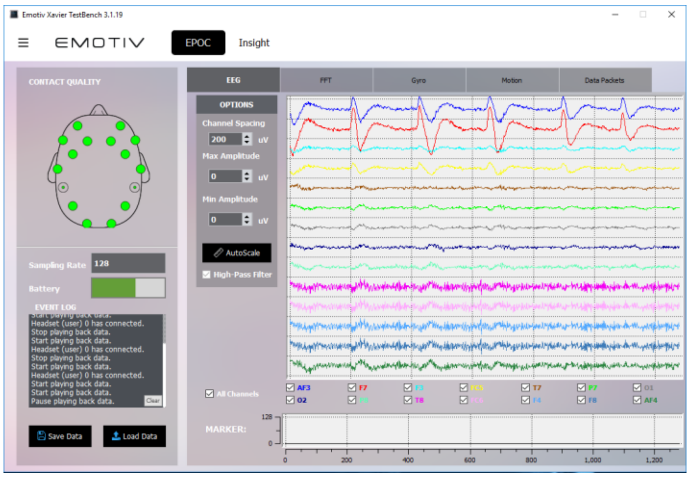

Figure 16 EEG signal readings for all 14 sensors of Emotiv Epoc+

Throughout the testing process, a single Emotiv test subject was used for the training and testing. In this way, parameters and configurations of the processing and features extraction were tailored for that particular test subject in the proposed system. Further trainings, signal analysis, tweaking and configurations are required for different users.

After the EEG signals were processed and features extracted using Matlab, OpenVibe and Emokey software, the user was able to command the wheel-chair to make basic movements. These basic movements included forward, reverse, left and right motions as well as standing and sitting positions of the wheel-chair. Other actuations signal can also be devised for any further improvements of the proposed system. The complete flow chart for the Arduino Mega board, which receives the data from the Intel based computer through serial port is presented in Figure 17. It is worthwhile to note here that climbing up the stairs is performed with the "backward" command and climbing down the stairs is performed with the same command. However, during these two processes the balance of the wheel-chair is of critical importance. This is performed using the IMU on board the controller and is the subject of another publication.

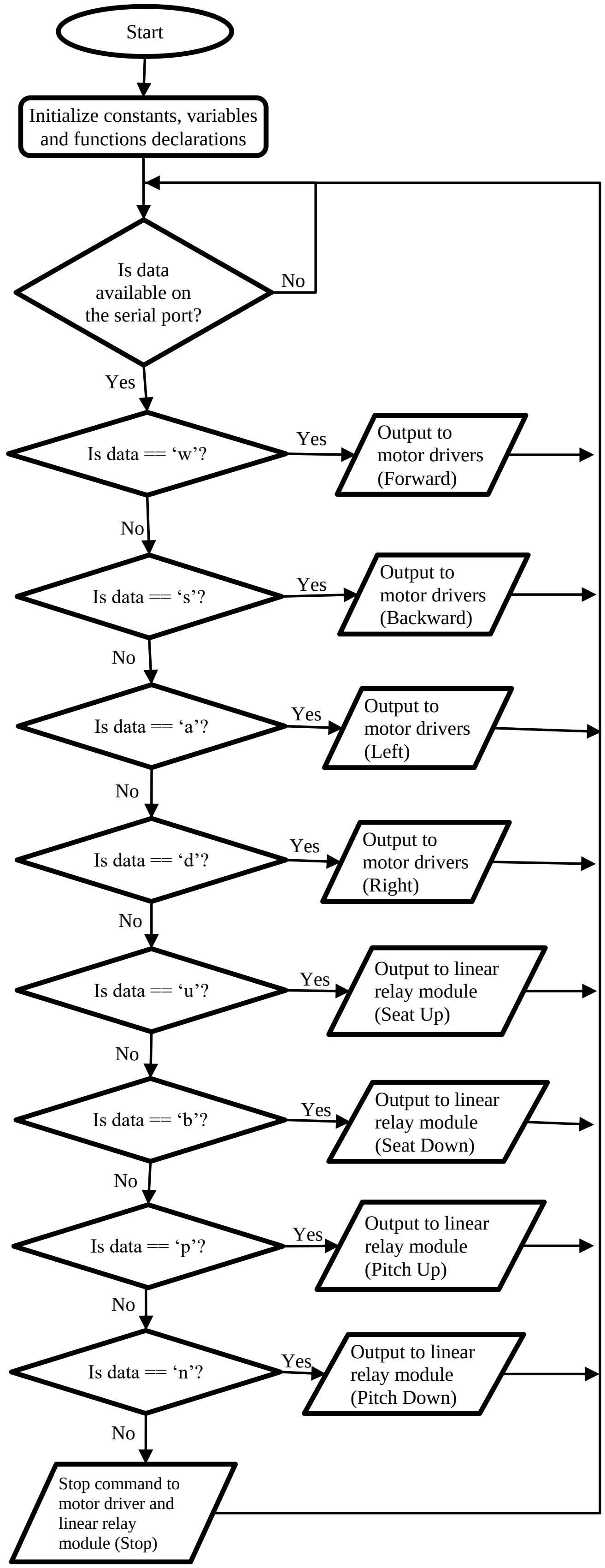

Figure 17 Arduino control flow chart

The wheel-chair was tested with a user of 78 kg (less than 120 kg as designed) without the solar panel at the beginning. The full charge of the two 12V-batteries lasted for about 3.1 hours of heavy use. However, it is worthwhile to note that not all motors and actuators operate at the same time. This implies that the diversity factor of the loads as mentioned above is much less than that of the design considerations made above which proved to be satisfactory for a prototype. Further improvements to the electronics, the PWM motor control circuit and the control technique would greatly improve the operating time of the proposed wheel-chair as compared to its cost.

After connecting the solar panels, the operation time of the chair under the same operating conditions as above, the time was extended for almost one extra hour. It is worthwhile to note that the solar panels are fixed horizontally and do not face the sun for some time. The solar panels can be made to move and automatically track the sun. This would improve the charging process of the batteries and will result in even longer operation time for the wheel-chair, which is the subject for future research.

Based on comparison with other research works [80], the proposed system provides the users with extra features such as an inclusion of solar power to provide extra working hours for the wheel-chair and increase the overall efficiency of the system. Compared to other designs and systems [81], the proposed system allows the user to use mental commands to transform the wheel-chair into three different configurations (sitting, standing and lying back as well as controlling the forward, reverse and turning motions).

The proposed system was built for human usage and so, safety precautions must be in place for the user. In the mechanical system, the driving motors are equipped with active-low motor brakes and clutch mechanism to prevent the user from unnecessary movements when there is an emergency. The electrical system was also equipped with safety components such as Schneider circuit breaker rated for a maximum 32 A to prevent current surge. Using relay modules, different components with varying power requirements are isolated to prevent burning-out circuits. The control system has safety feature in place inside the code to prevent random behaviour from causing system failure using the microcontroller interrupts. Furthermore, a multiple seat belts (for torso and legs) are to be installed to properly and securely strap the wheel-chair user to the chair in cases of emergency. This however was not installed in the proposed system as it was not considered part of the electrical and mechanical designs.

VI. Conclusion

This paper presented the mechanical design and construction of the solar-powered-rechargeable brain-controlled wheel-chair with signal acquisition, filtration, feature extraction, processing, and control methods. It also presented the control and electrical systems of the wheel-chair, which consisted of motor drivers and linear actuators. The wheel-chair is controlled, to help patients with motor paralysis, using EEG signals from the Emotiv Epoc+ brain wave sensor meant mostly for gaming purposes. Several combinations, from several electrodes of the 14 signals of the Emotiv Epoc+ sensor, were used to decide upon the desired action. An alternative Joystick input was also presented in the proposed system. Processing and control were all handled by an Intel based computer and an Arduino Mega 2560-R3 board. PID controllers and complementary filters were used leading to highly efficient wheel-chair. The operating time of the wheel-chair without solar panels was around 3.1 hours with the intrinsic batteries and a 78-kg test person.

The system used two 50-W solar panels fitted horizontally to the rooftop of the wheel-chair in order to trickle charge the battery of the wheel-chair and increase the operation time of the wheel-chair by approximately one hour during outdoor operation. Design constraints in electrical and mechanical systems were applied in order to generate an efficient economical product within a budget of approximately $2000.

Further improvements to the system are underway in order to improve the balance of the chair using the incorporated IMU during stair climbing and implement the control algorithm on a raspberry pi embedded system board with all the signal processing and data analysis and acquisition. Moreover, the solar panels fitted on top of the chair can be made to track the sun in order to improve its efficiency of electric power generation. These improvements would be the subject of another publication.

Acknowledgement

The authors wish to thank the Arab Academy for Science Technology and Maritime Transport (AASTMT) in Alexandria, Egypt, for supporting this research work along with the Egyptian Academy for Scientific Research and Technology. Moreover, the authors wish to thank their colleagues who participated in the manufacturing of the prototype, some design details and the logistics.

References

[1] M. B. I. Reaz, M. S. Hussain and F. Mohd-Yasin, “Techniques of EMG signal analysis: detection, processing, classification and Applications”, Biological procedures online, January 18, 2006, issue 8, pp. 11–35.

[2] J.J. Vidal, “Toward direct brain-computer communication”, Annual Review of Biophysics and Bioengineering, 1973, pp. 157–180.

[3] Peter Baranyi, Adam Csapo, “Definition and Synergies of Cognitive Infocommunications”, Acta Polytechnica Hungarica, 2012, Vol. 9 issue No. 1, pp. 67-83.

[4] Tan D., Nijholt A., “Brain-Computer Interfaces and Human-Computer Interaction.”, Human-Computer Interaction Series. Springer London, SN - 978-1-84996-272-8 UR, 2010.

[5] John S. Barlow, “EMG artifact minimization during clinical EEG recordings by special analog filtering”, Electroencephalography and clinical Neurophysiology, Issue 58 (2), February 17, 1984.

[6] Naveen.R. S and Anitha Julian, “Brain computer interface for wheel chair control”, IEEE – issue 31661, 4-6 July 2013.

[7] Niels Birbaumer, Ander Ramos Murguialdaya, and Leonardo Cohend, “Brain–computer interface in paralysis”, Current Opinion in Neurology, 2008, issue 21(6), pp 635-638.

[8] Nijboer F, Sellers E, Mellinger J, “A brain-computer interface in patients with amyotrophic lateral sclerosis.”, Clinical Neurophysiology, 2008, issue 119, pp. 1909–1916.

[9] Birbaumer N, Cohen L., “Brain-computer-interfaces (BCI): communicationand restoration of movement in paralysis.”, J Physios 2007; issue 579.3, pp. 621–636.

[10] Lebedev MA, Nicolelis MA., “Brain machine interfaces: past, present and future.”, Trends Neuroscience, 2006; issue 29, pp. 536–546.

[11] Sitaram R, Zhang H, Guan C, “Temporal classification of multichannel near-infrared spectroscopy signals of motor imagery for developing a brain-computer interface”, Neuroimage 2007; issue 34, pp. 1416–1427.

[12] Caria A, Veit R, Sitaram R, “Regulation of anterior insular cortex activity using real-time fMRI.”, Neuroimage 2007; Issue 35, pp. 1238–1246.

[13] Riehle A, Vaadia E, “Motor cortex in voluntary movements. A distributed system for distributed functions”, Boca Raton: CRC Press; 2005.

[14] Felton EA, Wilson JA, Williams JC, Garell PC., “Electrocorticographically controlled brain–computer interfaces using motor and sensory imagery in patients with temporary subdural electrode implants”, J Neurosurgery 2007; issue 106, pp. 495–500.

[15] Luis Fernando Nicolas-Alonso and Jaime Gomez-Gil “Brain Computer Interfaces, a Review”, sensors (basel), Published: 31 January 2012, issue 12(2), pp. 1211-1279.

[16] A. Eliseyev, C. Moro, T. Costecalde, N. Torres, S. Gharbi, C. Mestais, A. L. Benabid, T. Aksenova, “Iterative N-way PLS for self-paced BCI in freely moving animals.”, Journal of Neural Engineering, issue 8, 2011.

[17] D. Öngür, J.L. Price; “The Organization of Networks within the Orbital and Medial Prefrontal Cortex of Rats, Monkeys and Humans”, Cerebral Cortex, Volume 10, Issue 3, 1 March 2000, pp. 206–219.

[18] Baum, Michele (6 September 2008). "Monkey Uses Brain Power to Feed Itself with Robotic Arm". Pitt Chronicle. Retrieved 6 July 2009.

[19] Gaurav Sinha, Rahul Shahi, Mani Shankar., “Human Computer Interaction”, published by IEEE, Nov. 2010, 19-21.

[20] Polikov, Vadim S., Patrick A. Tresco, and William M. Reichert, "Response of brain tissue to chronically implanted neural electrodes", Journal of neuroscience methods, 2005.08.015, issue 148 (1), pp. 1-18.

[21] Gulati, Tanuj; Won, Seok Joon; Ramanathan, Dhakshin S.; Wong, Chelsea C.; Bodepudi, Anitha; Swanson, Raymond A.; Ganguly, Karunesh, "Robust Neuroprosthetic Control from the Stroke Perilesional Cortex", the Journal of Neuroscience, June 2015, Issue 35 (22), pp. 8653-8661.

[22] Serruya MD, Donoghue JP. “Chapter III: Design Principles of a Neuromotor Prosthetic Device”, Neuroprosthetics: Theory and Practice, ed. Kenneth W. Horch, Gurpreet S. Dhillon. Imperial College Press, 2003, pp. 1158-1196.

[23] Yanagisawa, Takafumi, "Electrocorticograpic Control of Prosthetic Arm in Paralyzed Patients", American Neurological Association, March 2011, issue 71(3), pp.353-361.

[24] Pei, X., "Decoding Vowels and Consonants in Spoken and Imagined Words Using Electrocorticographic Signals in Humans", Journal of Neural Engineering, August 2011, issue 8 (4): 046028

[25] Melissa González, Lochi Yu. “Auditory imagery classification with a non-invasive BCI”. Central American and Panama Convention (concapan xxxvi), IEEE, 2016, issue 36.

[26] Tonio Ball,Markus Kern,Isabella Mutschler,Ad Aertsen,Andreas Schulze-Bonhage, “Signal quality of simultaneously recorded invasive and non-invasive EEG”. Neuroimage, Elsevier, 1 July 2009, issue 46(3), pp. 708-716.

[27] http://www.solidworks.com/, “Dassault Systems SolidWorks Corporation” copyright 2017.

[28] https://www.arduino.cc/en/Main/arduinoBoardMega2560/, “Arduino – Arduino Mega 2560 - REV3”, copyright 2017.

[29] https://www.arduino.cc/, “Arduino”, copyright 2017 Arduino.

[30] Martin A. Green, Keith Emery, Yoshihiro Hishikawa, Wilhelm, Warta, Ewan D. Dunlop, “Solar cell efficiency”.

[31] Chetan Singh Solanki, “Solar Photovoltaic Technology and Systems: A Manual for Technicians, Trainers and Engineers,” PHI Learning, New Delhi, 2013.

[32] Ulanoff, L. Elon Musk and SolarCity unveil ‘world’s most efficient’ solar panel, Mashable, 2 October 2015, accessed 28 June 2016.

[33] I. Boldea, S.A. Nasar, “Linear electric actuators and generators,” IEEE, (18-21 May, 1997), Milwaukee, Wisonsin, USA.

[34] Robert L. Norton, “Machine design, an integrated approach,” Pearson, Massachusetts, fifth edition, 2014.

[35] John J. Grainger and William D. Stevenson, “Power System Analysis,” McGraw-Hill, New York, 2011.

[36] James Larminie and Johns Lowry, “Electric Vehicle Technology Explained,” John Wiley & Sons, New Jersey, 2012.

[37] Proflex; “Crystalline silicon terrestrial photovoltaic (PV) modules – Design qualification and type approval Reference”, International Standard IEC61215.

[38] Michael Boxwell, “Solar Electricity Handbook: A Simple, Practical Guide to Solar Energy - Designing and Installing Photovoltaic Solar Electric Systems,” Greenstream Publishing, Coventry, 2010.

[39] Martin Sokol, Didac Mallorquin Colina, Nikos Konstantinidis, Ahmed Berrada, “MPPT Tracker S.M.K.B. Edition: European Project Semester thesis,” Ecole Nationale d'Ingénieurs de Tarbes, Tarbes, 2010.

[40] Mark Hankins, “Stand-alone Solar Electric Systems: The Earthscan Expert Handbook for Planning, Design and Installation”. Earthscan, London, 2010.

[41] Rehan Jamil, “Maximum Power Point Tracker (MPPT) Based Photovoltaic (PV) Water Pumping System Using AC and DC Motors”. GRIN Verlag, München, 2014.

[42] Ernst Niedermeyer, F. H. Lopes da Silva, “Electroencephalography: Basic Principles, Clinical Applications, and Related Fields,” Lippincott Williams & Wilkins, Pennsylvania, 2005.

[43] Kylie J Barnett, “Colour knowledge: The role of the right hemisphere in colour processing and object colour knowledge. Laterality,” National Center for biotechnology information and U.S. National library of medicine, Maryland, 2008.

[44] http://neurosky.com/biosensors/eeg-sensor/biosensors/, Neurosky, 2012.

[45] https://store.choosemuse.com/products/muse/, Neurosky, 2012.

[46] https://www.emotiv.com/, Emotiv, 2011

[47] Saleh Ibrahim Alzahrani, “p300 wave detection using emotiv epoc+ headset: effects of matrix size, flash duration, and colors,” ProQuest, Michigan, Fall 2016.

[48] Kamel Nidal, Aamir Saeed Malik, “EEG/ERP Analysis: Methods and Applications,” CRC Press, Boca Raton, 2014.

[49] Maurizio Di Paolo Emilio, “Embedded Systems Design for High-Speed Data Acquisition and Control,” Springer, New York, 2014

[50] Saeid Sanei, “Adaptive processing of brain signal,” John Wiley & Sons, New Jersey, 2013.

[51] Ivo K¨athner, Selina C Wriessnegger, Gernot R M¨uller-Putz, Andrea K¨ubler, and Sebastian Halder, “Effects of mental workload and fatigue on the p300, alpha and thetaband power during operation of an ERP (P300) brain–computer interface,” National Center for biotechnology information and U.S. National library of medicine, 2014.

[52] SC Kleih, F Nijboer, S Halder, and A Kubler, “Motivation modulates the p300 amplitude during brain–computer interface use”, Clinical Neurophysiology, 121 (7), pp. 1023–1031, 2010.

[53] H´el`ene Otzenberger, Daniel Gounot, and JR Foucher, “Optimisation of a post-processing method to remove the pulse artifact from eeg data recorded during fmri: an application to p300 recordings during e-fmri”, Neuroscience research, 57 (2), pp. 230–239, 2007

[54] Pedro Campos,Nicholas Graham, Joaquim Jorge, Nuno Nunes, Philippe Palanque, Marco Winckler, “Human-Computer Interaction ”, New York: Springer, 2011.

[55] Emotiv Epoc+ Manual: https://emotiv.zendesk.com/hc/en-us/article_attachments/200343895/EPOCUserManual2014.pdf, Emotiv systems, 2014.

[56] Pritom Chowdhury, S. S. Kibria Shakim, Md Risul Karim,Md Khalilur Rhaman "Cognitive efficiency in robot control by Emotiv EPOC" Informatics, Electronics & Vision (ICIEV) 2014 International Conference, 23-24 May 2014.

[57] E.T. McAdams, J. Jossinet, R. Subramanian, R.G.E. McCauley "Characterization of gold electrodes in phosphate buffered saline solution by impedance and noise measurements for biological applications", Engineering in Medicine and Biology Society, 2006. EMBS'06. 28th Annual International Conference of the IEEE, 30 Aug.-3 Sept. 2006.

[58] Debener S, Minow F, Emkes R, Gandras K, de Vos M," How about taking a low-cost, small, and wireless EEG for a walk?" Psychophysiology, 2012, 49(11):1617–1621.

[59] Rabiner, L. R.; Gold, B. "Theory and application of digital signal processing". Englewood Cliffs, N.J., Prentice-Hall, Inc., 1975. 777 p

[60] Gabriel Pires, Urbano Nunes, and Miguel Castelo-Branco, "Statistical spatial filtering for a p300-based bci: tests in able-bodied, and patients with cerebral palsy and amyotrophic lateral sclerosis", Journal of neuroscience methods, 195 (2), pp. 270–281, 2011.

[61] I. Selesnick, "Introduction to Sparsity in Signal Processing, Connexions", Web site: http://cnx.org/content/m43545/, May 27, 2012.

[62] Dean J Krusienski, Eric W Sellers, François Cabestaing, Sabri Bayoudh, Dennis J McFarland, Theresa M Vaughan and Jonathan R Wolpaw. "A comparison of classification techniques for the P300 Speller" Journal of Neural Engineering, Volume 3, Number 4, Published 26 October 2006.

[63] D.J. Krusienski,E.W, Sellers,D.J, McFarland,T.M, Vaughan,J.R, Wolpaw, "Toward enhanced P300 speller performance" Journal of Neuroscience Methods, 15 January 2008.

[64] Kun Li, Ravi Sankar, Yael Arbel, Emanuel Donchin, "Single trial independent component analysis for P300 BCI system" EMBC Annual International Conference of the IEEE, 3-6 Sept. 2009.

[65] M. Kaper, P. Meinicke, U. Grossekathoefer. "BCI competition 2003-data set IIb: support vector machines for the P300 speller paradigm" IEEE, 24 May 2004.

[66] S M Abdullah-Al-Mamun, "A novel algorithm for Emotiv EPOC spellers based on Emokey", Clinical Neurophsyology, november 2014.

[67] Yann Renard, Fabien Lotte, Guillaume Gibert, Marco Congedo "OpenViBE: An Open-Source Software Platform to Design, Test, and Use Brain–Computer Interfaces in Real and Virtual Environments" Presence: Teleoperators and Virtual Environments, Volume 19, Issue 1, February 2010, p.35-53.

[68] H. Mirghasemi, R. Fazel-Rezai, M. B. Shamsollahi, "Analysis of P300 Classifiers in Brain Computer Interface Speller" IEEE, 30 Aug.-3 Sept. 2006.

[69] L. Vega-Escobar, A. E. Castro-Ospina, L. Duque-Muñoz, "Feature extraction schemes for BCI systems", 20th Symposium on Signal Processing Images and Computer Vision (STSIVA) 2015, pp. 1-6, 2015.

[70] A Chamanzar, M Shabany, A Malekmohammadi, S Mohammadinejad "Efficient Hardware Implementation of Real-Time Low-Power Movement Intention Detector System Using FFT and Adaptive Wavelet Transform", Published in: IEEE Transactions on Biomedical Circuits and Systems Volume: 99, June 2017.

[71] Fabien Lotte, Marco Congedo, Anatole Lecuyer, Fabrice Lamarche, Bruno Arnaldi, "A review of classification algorithms for EEG-based brain computer interfaces" Journal of Neural Engineering, IOP Publishing, 2007, Issue 4, pp.24.

[72] Preeti Sharma, Santvana Vats, "Brain computer interface" UG, Department of Electronics and Communication Engineering, Raj Kumar Goel Institute of Technology for Women, UP, India.

[73] A. Materka, M. Byczuk, "Using Comb Filter to Enhance SSVEP for BCI Applications" MEDSIP, 2006, IET 3rd International Conference.

[74] Na Lu, Tengfei Li, Xiaodong Ren, Hongyu Miao, "A Deep Learning Scheme for Motor Imagery Classification based on Restricted Boltzmann Machines", IEEE Transactions on Neural Systems and Rehabilitation Engineering,VOLUME: 25, Issue: 6, June 2017.

[75] Begg, Rezaul, "Neural Networks in Healthcare: Potential and Challenges: Potential", Idea Group Publishing, 2006,ISBN 1591408504 .

[76] Md. Shakhawat Hossain, Simanto Saha, Md. Ahasan Habib, Abdullah Al Noman, Takia Sharfuddin, Khawza I. Ahmed, "Application of wavelet-based maximum entropy on the mean in channel optimization for BCI", Medical Engineering, Health Informatics and Technology (MediTec), 2016 International Conference.

[77] Emotiv Tools: XavierEmoKey from Emotiv official website, https://emotiv.zendesk.com/hc/en-us/articles/201453885-Emotiv-Xavier-Tools-XavierEmoKey, Emotiv systems.

[78] C. Guger, A. Schlogl, C. Neuper, D. Walterspacher, T. Strein, G. Pfurtscheller, "Rapid prototyping of an EEG-based brain-computer interface (BCI)", IEEE Transactions on Neural Systems and Rehabilitation Engineering, Volume: 9, Issue: 1, March 2001.

[79] Yann Renard, Fabien Lotte, Guillaume Gibert, Marco Congedo, Emmanuel Maby, Vincent Delannoy, Olivier Bertrand, Anatole Lécuyer, "OpenViBE: An Open-Source Software Platform to Design, Test, and Use Brain–Computer Interfaces in Real and Virtual Environments", Presence Volume: 19, Issue: 1, Feb. 1 2010.

[80] D. W. K. Ng, Y. W. Soh, S. Y. Goh, "Development of an autonomous BCI wheelchair", Computational Intelligence in Brain ComputerInterfaces (CIBCI) 2014 IEEE Symposium, pp. 1-4, Dec 2014.

[81] R. S. Naveen, A. Julian, "Brain computing interface for wheel chair control", Fourth International Conference on Computing Communications and Networking Technologies (ICCCNT), pp. 1-5, 2013.